



HAL
open science

Measuring the porosity and the tortuosity of porous materials via reflected waves at oblique incidence

Zine El Abiddine Fellah, S Berger, W Lauriks, C Depollier, C Aristégui, J-Y Chapelon

► **To cite this version:**

Zine El Abiddine Fellah, S Berger, W Lauriks, C Depollier, C Aristégui, et al.. Measuring the porosity and the tortuosity of porous materials via reflected waves at oblique incidence. *Journal of the Acoustical Society of America*, 2003, 113, pp.2424 - 2433. 10.1121/1.1567275 . hal-04230399

HAL Id: hal-04230399

<https://hal.science/hal-04230399>

Submitted on 5 Oct 2023

HAL is a multi-disciplinary open access archive for the deposit and dissemination of scientific research documents, whether they are published or not. The documents may come from teaching and research institutions in France or abroad, or from public or private research centers.

L'archive ouverte pluridisciplinaire **HAL**, est destinée au dépôt et à la diffusion de documents scientifiques de niveau recherche, publiés ou non, émanant des établissements d'enseignement et de recherche français ou étrangers, des laboratoires publics ou privés.

Measuring the porosity and the tortuosity of porous materials via reflected waves at oblique incidence

Z. E. A. Fellah

National Institute of Health and Medical Research (INSERM U556), 151 cours Albert Thomas,
69424 Lyon Cedex 03, France

S. Berger and W. Lauriks

Laboratorium voor Akoestiek en Thermische Fysica, Katholieke Universiteit Leuven, Celestijnenlaan 200 D,
B-3001 Heverlee, Belgium

C. Depollier

Laboratoire d'Acoustique de l'Université du Maine, UMR-CNRS 6613, Université du Maine,
Avenue Olivier Messiaen, 72085 Le Mans Cedex 09, France

C. Aristégui and J.-Y. Chapelon

National Institute of Health and Medical Research (INSERM U556), 151 cours Albert Thomas,
69424 Lyon Cedex 03, France

(Received 31 October 2002; revised 21 February 2003; accepted 24 February 2003)

An ultrasonic reflectivity method is proposed for measuring porosity and tortuosity of porous materials having a rigid frame. Porosity is the relative fraction by volume of the air contained within a material. Tortuosity is a geometrical parameter which intervenes in the description of the inertial effects between the fluid filled the porous material and its structure at high frequency range. It is generally easy to evaluate the tortuosity from transmitted waves, this is not the case for porosity because of its weak sensitivity in transmitted mode. The proposed method is based on measurement of reflected wave by the first interface of a slab of rigid porous material. This method is obtained from a temporal model of the direct and inverse scattering problems for the propagation of transient ultrasonic waves in a homogeneous isotropic slab of porous material having a rigid frame [Z. E. A. Fellah, M. Fellah, W. Lauriks, and C. Depollier, *J. Acoust. Soc. Am.* **113**, 61 (2003)]. Reflection and transmission scattering operators for a slab of porous material are derived from the responses of the medium to an incident acoustic pulse at oblique incidence. The porosity and tortuosity are determined simultaneously from the measurements of reflected waves at two oblique incidence angles. Experimental and numerical validation results of this method are presented. © 2003 Acoustical Society of America. [DOI: 10.1121/1.1567275]

PACS numbers: 43.20.Bi, 43.20.Hq [ANN]

I. INTRODUCTION

The ultrasonic characterization of porous materials saturated by airlike plastic foams, fibrous, or granular materials is of a great interest for a wide range of industrial applications. These materials are frequently used in the automotive and aeronautics industries or in the building trade. The determination of the properties of a medium from waves that have been reflected by or transmitted through the medium is a classical inverse scattering problem. Such problems are often approached by taking a physical model of the scattering process, generating a synthetic response for some assumed values of the parameters, adjusting these parameters until reasonable agreement is obtained between the synthetic response and the observed data. Two important parameters which appear in theories of sound propagation in porous materials¹⁻¹³ are the porosity and the tortuosity. Porosity is the relative fraction, by volume, of air contained in the connected pores in the material. Unlike other parameters included in the description of different various phenomena occurring in the acoustical propagation of porous material at high frequency range such as tortuosity,¹¹ viscous characteristic length,⁵ and thermal characteristic length,¹² or in the

low frequency range such as flow resistivity¹¹ and thermal permeability,¹³ the porosity is a key parameter playing an important role in the propagation at all frequencies. As such, in studies of acoustical properties of porous materials, it is highly desirable to be able to measure this parameter.

Beranek¹⁰ described an apparatus (porosimeter) used to measure the porosity of porous materials. This device was based on the equation of state for ideal gases at constant temperature (i.e., Boyle's law). Porosity can be determined by measuring the change in air pressure occurring with a known change in volume of the chamber containing the sample. In the Beranek apparatus, both pressure change and volume change are monitored using a U-shaped fluid-filled manometer. An alternate technique for measuring porosity is a dynamic method proposed by Leonard.¹⁴ Techniques that use water as the pore-filling fluid, rather than air, are common in geophysical studies.^{15,16} Mercury has been used as the pore-filling fluid in other applications.¹⁷ However, for many materials, the introduction of liquids into the material is not appropriate. Recently a similar device to that of Beranek, involving the use of an electronic pressure transducer, was introduced by Champoux *et al.*¹⁸ This device can be

used to measure very slight changes in pressure accurately, and the output can be recorded by a computer.

The tortuosity α_∞ , namely the structure factor k_s by Zwikker and Kosten,¹¹ or the parameter q^2 by Attenborough,⁹ is an important parameter which intervenes in the description of the inertial interaction between the fluid and the structure in the porous material at high frequency range. In the case of cylindrical pores making an angle ϑ with the direction of propagation, $\alpha_\infty = 1/\cos^2 \vartheta$. The tortuosity can be evaluated by electrical measurements,¹⁶ or by using a superfluid ⁴He as the pore fluid.⁵ It can also be evaluated by acoustical techniques as an ultrasonics measurement of transmitted waves.^{1,3,4,19}

In this work, we present a method of measuring the porosity and the tortuosity from the measurement of acoustic wave reflected by a slab of porous material at oblique incidence. This method is based on a temporal model of the direct and inverse scattering problems for the propagation of transient ultrasonic waves in a homogeneous isotropic slab of porous material having a rigid frame initially introduced by two of the authors (Z.E.A.F and C.D) in Refs. 1–4. The viscous and thermal losses of the medium are described by the Johnson *et al.*⁵ and Allard⁶ model modified by a fractional calculus based method in order to be used in time domain. Reflection and transmission scattering operators of a slab of porous material are derived for an oblique incidence and thus the responses of the medium to an incident acoustic pulse are obtained.

The outline of this paper is as follows. In Sec. II, a time domain model is given, and the basic equations of wave propagation in porous material are written for an oblique incidence. Section III is devoted to the direct problem and to the expressions of the reflection and transmission kernels in the time domain at oblique incidence. Finally in Sec. IV, an experimental validation with ultrasonic measurement is treated for two plastic foams having different values of flow resistivity. The porosity and tortuosity are measured via reflected waves for different incidence angles.

II. MODEL

In the acoustics of porous materials, a distinction can be made between two situations depending on whether the frame is moving or not. In the first case, the dynamics of the waves due to the coupling between the solid frame and the fluid are clearly described by the Biot theory.^{7,8} In air-saturated porous media the structure is generally motionless and the waves propagate only in the fluid. This case is described by the model of equivalent fluid which is a particular case in the Biot model, in which the interactions between the fluid and the structure are taken into account in two frequency response factors: the dynamic tortuosity of the medium $\alpha(\omega)$ given by Johnson *et al.*⁵ and the dynamic compressibility of the air included in the porous material $\beta(\omega)$ given by Allard.⁶ In the frequency domain, these factors multiply the density of the fluid and its compressibility respectively and represent the deviation from the behavior of the fluid in free space as the frequency increases. In the time

domain, they act as operators and in the asymptotic domain (high frequency approximation) their expressions are given¹⁻⁴ by

$$\tilde{\alpha}(t) = \alpha_\infty \left(\delta(t) + \frac{2}{\Lambda} \left(\frac{\eta}{\pi \rho_f} \right)^{1/2} t^{-1/2} \right), \quad (1)$$

$$\tilde{\beta}(t) = \left(\delta(t) + \frac{2(\gamma-1)}{\Lambda'} \left(\frac{\eta}{\pi P_r \rho_f} \right)^{1/2} t^{-1/2} \right). \quad (2)$$

In these equations, $\delta(t)$ is the Dirac function, Pr is the Prandtl number, η and ρ_f are, respectively, the fluid viscosity and the fluid density, and γ is the adiabatic constant. The relevant physical parameters of the model are the tortuosity of the medium α_∞ initially introduced by Zwikker and Kosten,¹¹ the viscous and the thermal characteristic lengths Λ and Λ' introduced by Johnson *et al.*⁵ and Allard.⁶ In this model the time convolution of $t^{-1/2}$ with a function is interpreted as a semi derivative operator following the definition of the fractional derivative of order ν given in Samko and colleagues²⁰

$$D^\nu[x(t)] = \frac{1}{\Gamma(-\nu)} \int_0^t (t-u)^{-\nu-1} x(u) du, \quad (3)$$

where $\Gamma(x)$ is the Gamma function.

In this framework, the basic equations of our model can be written as

$$\rho_f \tilde{\alpha}(t) * \frac{\partial v_i}{\partial t} = -\nabla_i p \quad \text{and} \quad \frac{\tilde{\beta}(t)}{K_a} * \frac{\partial p}{\partial t} = -\nabla \cdot \mathbf{v}, \quad (4)$$

where $*$ denotes the time convolution operation, p is the acoustic pressure, \mathbf{v} is the particle velocity, and K_a is the bulk modulus of air. The first equation is the Euler equation, the second one is the constitutive equation.

For a wave propagating at oblique incidence in the plane (xoz) and making an angle θ along the x -axis, these equations become

$$\begin{aligned} \rho_f \alpha_\infty \frac{\partial v_x(x,z,t)}{\partial t} + \frac{2\rho_f \alpha_\infty}{\Lambda} \left(\frac{\eta}{\pi \rho_f} \right)^{1/2} \int_0^t \frac{\partial v(x,z,t')/\partial t'}{\sqrt{t-t'}} dt' \\ = -\frac{\partial p(x,z,t)}{\partial x}, \\ \rho_f \alpha_\infty \frac{\partial v_z(x,z,t)}{\partial t} + \frac{2\rho_f \alpha_\infty}{\Lambda} \left(\frac{\eta}{\pi \rho_f} \right)^{1/2} \int_0^t \frac{\partial v(x,z,t')/\partial t'}{\sqrt{t-t'}} dt' \\ = -\frac{\partial p(x,z,t)}{\partial z}, \\ \frac{1}{K_a} \frac{\partial p(x,z,t)}{\partial t} + \frac{2(\gamma-1)}{K_a \Lambda'} \left(\frac{\eta}{\pi \rho_f P_r} \right)^{1/2} \int_0^t \frac{\partial p(x,z,t')/\partial t'}{\sqrt{t-t'}} dt' \\ = -\frac{\partial v(x,z,t)}{\partial x} - \frac{\partial v(x,z,t)}{\partial z}, \end{aligned} \quad (5)$$

where v_x , v_z are the components of the particle velocity along the axes x' and z .

In these equations, the convolutions express the dispersive nature of the porous material. They take into account the

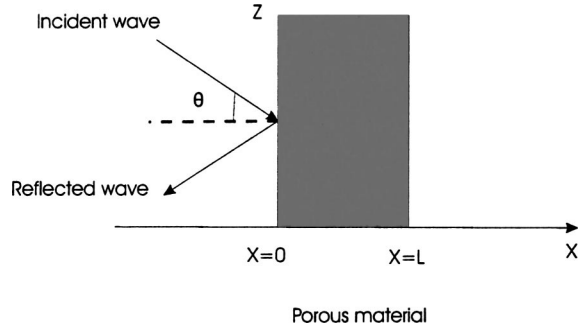


FIG. 1. Geometry of the problem.

memory effects due to the fact that the response of the medium to the wave excitation is not instantaneous but needs more time to take effect.

III. DIRECT PROBLEM

The direct scattering problem is that of determining the scattered field as well as the internal field, that arises when a known incident field impinges on the porous material with known physical properties. To compute the solution of the direct problem one needs to know the Green's function³ of the modified wave equation in the porous medium. In that case, the internal field is given by the time convolution of the Green's function with the incident wave, and the reflected and transmitted fields are deduced from the internal field and the boundary conditions. In this section some notation is introduced. The geometry of the problem is shown in Fig. 1. A homogeneous porous material occupies the region $0 \leq x \leq L$. This medium is assumed to be isotropic and to have a rigid frame. A short sound pulse impinges at oblique incidence on the medium from the left, it gives rise to an acoustic pressure field $p(x, z, t)$ and an acoustic velocity field $\mathbf{v}(x, z, t)$ within the material, which satisfying the system of Eqs. (5), which can be written as

$$a \frac{\partial v_x(x, z, t)}{\partial t} + b \frac{\partial^{1/2} v_x(x, z, t)}{\partial t^{1/2}} = - \frac{\partial p(x, z, t)}{\partial x}, \quad (6)$$

$$a \frac{\partial v_z(x, z, t)}{\partial t} + b \frac{\partial^{1/2} v_z(x, z, t)}{\partial t^{1/2}} = - \frac{\partial p(x, z, t)}{\partial z}, \quad (7)$$

$$d \frac{\partial p(x, z, t)}{\partial t} + f \frac{\partial^{1/2} p(x, z, t)}{\partial t^{1/2}} = - \frac{\partial v_x(x, z, t)}{\partial x} - \frac{\partial v_z(x, z, t)}{\partial z}. \quad (8)$$

with

$$a = \rho_f \alpha_\infty, \quad b = \frac{2\rho_f \alpha_\infty}{\Lambda} \left(\frac{\eta}{\rho_f} \right)^{1/2},$$

$$d = \frac{1}{K_a} \quad \text{and} \quad f = \frac{2(\gamma-1)}{K_a \Lambda'} \left(\frac{\eta}{\rho_f P_r} \right)^{1/2}.$$

In the region $x \leq 0$, the incident pressure wave is given by

$$p^i(x, z, t) = p^i \left(t - \frac{x \cos \theta}{c_0} - \frac{z \sin \theta}{c_0} \right), \quad (9)$$

where c_0 is the velocity of the free fluid ($x \leq 0$); $c_0 = \sqrt{K_a / \rho_f}$.

In the region $0 \leq x \leq L$, the pressure wave is given by

$$p^i(x, z, t) = p^i \left(t - \frac{x \cos \theta'}{c'} - \frac{z \sin \theta'}{c'} \right), \quad (10)$$

where c' is the velocity in the porous material ($0 \leq x \leq L$), and the refraction angle θ' is given by the Descartes-Snell law:⁶

$$\frac{\sin \theta}{c_0} = \frac{\sin \theta'}{c'}. \quad (11)$$

To simplify the system of equations (5), we can then use the following property:

$$\frac{\partial}{\partial z} = - \frac{\sin \theta}{c_0} \frac{\partial}{\partial t}, \quad (12)$$

which implies

$$\frac{\partial v_z}{\partial z} = - \frac{\sin \theta}{c_0} \frac{\partial v_z}{\partial t} \quad \text{and} \quad \frac{\partial p}{\partial z} = - \frac{\sin \theta}{c_0} \frac{\partial p}{\partial t}. \quad (13)$$

From Eqs. (7) and (13), we obtain then the relation

$$\frac{\partial v_z}{\partial z} = - \frac{\sin^2 \theta}{c_0^2} \left(a + b \frac{\partial^{-1/2}}{\partial t^{-1/2}} \right)^{-1} * \frac{\partial p}{\partial t}. \quad (14)$$

By using Eqs. (6), (8), and (14), the equation system (6), (7) and (8) can thus be simplified to

$$a \frac{\partial v_x(x, z, t)}{\partial t} + b \frac{\partial^{1/2} v_x(x, z, t)}{\partial t^{1/2}} = - \frac{\partial p(x, z, t)}{\partial x}, \quad (15)$$

$$d \frac{\partial p(x, z, t)}{\partial t} + f \frac{\partial^{1/2} p(x, z, t)}{\partial t^{1/2}} = - \frac{\partial v_x(x, z, t)}{\partial x} + \frac{\sin^2 \theta}{c_0^2} \left(a + b \frac{\partial^{-1/2}}{\partial t^{-1/2}} \right)^{-1} * \frac{\partial p(x, z, t)}{\partial t}. \quad (16)$$

From Eqs. (15) and (16), we derive the generalized lossy wave equation in the time domain along the x -axis

$$\frac{\partial^2 p(x, z, t)}{\partial x^2} - A \frac{\partial^2 p(x, z, t)}{\partial t^2} - B \frac{\partial^{3/2} p(x, z, t)}{\partial t^{3/2}} - C \frac{\partial p(x, z, t)}{\partial t} = 0, \quad (17)$$

where the coefficients A , B and C are constants, respectively, given by

$$A = \frac{1}{c_0^2} (\alpha_\infty - \sin^2 \theta), \quad B = \frac{2\alpha_\infty}{K_a} \sqrt{\frac{\rho_f \eta}{\pi}} \left(\frac{1}{\Lambda} + \frac{\gamma-1}{\sqrt{\text{Pr} \Lambda'}} \right),$$

and

$$C = \frac{4\alpha_\infty(\gamma-1)\eta}{K_a \Lambda \Lambda' \sqrt{\text{Pr}}}.$$

The first one is related to the velocity of the projected wave along the x -axis $c = c_0 / \sqrt{\alpha_\infty - \sin^2 \theta}$. The other coefficients are essentially dependent on the characteristic lengths Λ and Λ' , and express the viscous and thermal interactions between the fluid and the structure. The constant B governs the spreading of the signal while C is responsible of the attenuation of the wave. Obviously, a knowledge of these three coefficients allows the determination of the parameters α_∞ , Λ , and Λ' . One way to solve Eq. (17) with suitable initial and boundary conditions is by using the Laplace transform. The approach is quite simple although the inverse Laplace transform requires tedious calculi.³ A suitable setting for the introduction of the time domain solution of the modified wave propagation equation (17) is provided by the following model.

If the incident sound wave is launched in the region $x \leq 0$, then the expression of the pressure field in the region at the left of the material is the sum of the incident and reflected fields

$$p_1(x, t) = p^i \left(t - \frac{x \cos \theta}{c_0} \right) + p^r \left(t + \frac{x \cos \theta}{c_0} \right), \quad x < 0. \quad (19)$$

Here, $p_1(x, t)$ is the field in the region $x < 0$, p^i and p^r denote the incident and the reflected fields, respectively. In addition, a transmitted field is produced in the region at the right of the material. This has the form

$$p_3(x, t) = p^t \left(t - \frac{L}{c} - \frac{(x-L) \cos \theta}{c_0} \right), \quad x > L \quad (20)$$

[$p_3(x, t)$ is the field in the region $x > L$ and p^t is the transmitted field].

The incident and scattered fields are related by the scattering operators (i.e., the reflection and transmission operators) for the material. These are integral operators represented by

$$\begin{aligned} p^r(x, t) &= \int_0^t \tilde{R}(\tau) p^i \left(t - \tau + \frac{x}{c_0} \right) d\tau \\ &= \tilde{R}(t) * p^i(t) * \delta \left(t + \frac{x \cos \theta}{c_0} \right), \end{aligned} \quad (21)$$

$$\begin{aligned} p^t(x, t) &= \int_0^t \tilde{T}(\tau) p^i \left(t - \tau - \frac{L}{c} - \frac{(x-L)}{c_0} \right) d\tau \\ &= \tilde{T}(t) * p^i(t) * \delta \left(t - \frac{L}{c} - \frac{(x-L) \cos \theta}{c_0} \right). \end{aligned} \quad (22)$$

In Eqs. (21) and (22) the functions \tilde{R} and \tilde{T} are the reflection and transmission kernels, respectively, for incidence from the left. Note that the lower limit of integration in Eqs. (21) and (22) is chosen to be 0, which is equivalent to assume that the incident wave front first impinges on the material at $t=0$.

The scattering operators given in Eqs. (21) and (22) are independent of the incident field used in the scattering experiment and depend only on the properties of the materials.

To derive the reflection and transmission coefficients, the boundary conditions of the flow velocity at the interfaces $x=0$ and $x=L$ are needed.¹ Using the same calculus steps

given in Ref. 1, we obtain the reflection and transmission scattering operators for a slab of porous material at oblique incidence

$$\begin{aligned} \tilde{R}(t) &= \left(\frac{1-E}{1+E} \right) \sum_{n \geq 0} \left(\frac{1-E}{1+E} \right)^{2n} \\ &\quad \times \left[F \left(t, 2n \frac{L}{c} \right) - F \left(t, (2n+2) \frac{L}{c} \right) \right], \end{aligned} \quad (23)$$

$$\tilde{T}(t) = \frac{4E}{(1+E)^2} \sum_{n \geq 0} \left(\frac{1-E}{1+E} \right)^{2n} F \left(t + \frac{L}{c_0}, (2n+1) \frac{L}{c} \right), \quad (24)$$

with

$$E = \frac{\phi \sqrt{1 - \frac{\sin^2 \theta}{\alpha_\infty}}}{\sqrt{\alpha_\infty \cos \theta}}. \quad (25)$$

These expressions take into account the n -multiple reflection in the material.

In most cases of porous materials saturated by air, the multiple reflection effects can be negligible because of the high attenuation of sound waves in these media. This depends on the thickness L and the flow resistivity σ of the porous material.

In the case where the multiple reflections can be neglected, the kernel of transmission is given by

$$\tilde{T}(t) = \frac{4E}{(1+E)^2} F \left(t + \frac{L}{c}, \frac{L}{c} \right),$$

and the kernel of reflection by

$$\tilde{R}(t) = r(t) + \mathfrak{R}(t), \quad (26)$$

with

$$r(t) = \left(\frac{1-E}{1+E} \right) \delta(t)$$

and

$$\mathfrak{R}(t) = - \frac{4E(1-E)}{(1+E)^3} F \left(t, \frac{2L}{c} \right). \quad (27)$$

$r(t)$ is the instantaneously response of the porous material corresponding to the reflection contribution at the first interface ($x=0$).

In the case of a semi-infinite medium when $L \rightarrow \infty$, it can be shown¹ that $F(t, 2L/c) \rightarrow 0$ and $\tilde{R}(t) \rightarrow r(t)$. This means that $\mathfrak{R}(t)$ is equivalent to the reflection at the rear interface ($x=L$), which is the bulk contribution to the reflection. The part of the wave corresponding to $r(t)$ is not subjected to the dispersion but is simply multiplied by the factor $(1-E)/(1+E)$. This shows that although tortuosity is a bulk parameter, it may be evaluated from the wave reflected at the first interface when the porosity is known and vice versa. Although generally speaking it is easy to evaluate the tortuosity from transmitted waves^{1,3,4,19,21} this is not the case for porosity because of its weak sensitivity in transmitted mode.¹ Figure 2 shows two simulated transmitted signals for a plastic foam M1. The first one (solid line) corresponds to the value

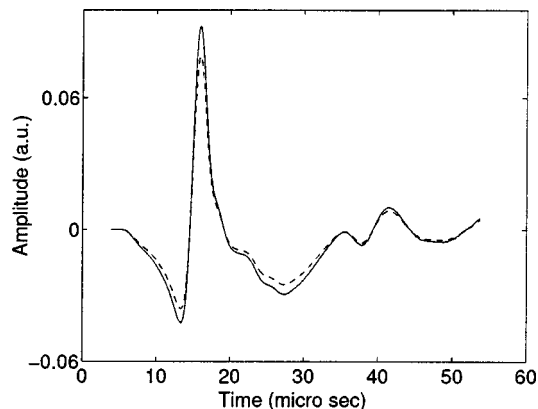


FIG. 2. Transmitted simulated signals for $\phi=0.98$ (solid line) and for $\phi=0.49$ (dashed line).

of porosity $\phi_1=0.98$ and the second one (dashed line) corresponds to $\phi_2=0.49$. The parameters of the plastic foam M1 (thickness 1.1 cm, $\phi=0.92$, $\alpha_\infty=1.25$, $\Lambda=50 \mu\text{m}$ and $\Lambda'=150 \mu\text{m}$, flow resistivity $\sigma=38\,000 \text{ Nm}^{-4} \text{ s}$) have been determined using conventional methods.^{1,3,4,19,21} Readers can see the slight difference between the two curves for a 50% difference in porosity values, which is due to the dispersion phenomenon that is governed by viscous, thermal and inertial effects contributed by α_∞ , Λ and Λ' and plays a more important role in the Green function $F(t,k)$ than ϕ .

In Fig. 3 we show by numerical simulation, the difference between the reflected wave at the first interface and the total reflected wave. The difference between the two curves is marginal. This means that the wave reflected by the slab may be approximated by the reflected wave by the first interface $r(t)$ with a good level of accuracy. It is easy to verify that this approximation is valid for any incidence angle θ . In the next section, we will show, by a simple measurements, how it is the possible to determine the porosity and the tortuosity by measuring reflected wave by a slab of porous material.

IV. ULTRASONIC MEASUREMENT

In this section, we measure the tortuosity and the porosity knowing the reflection coefficient at the first interface for

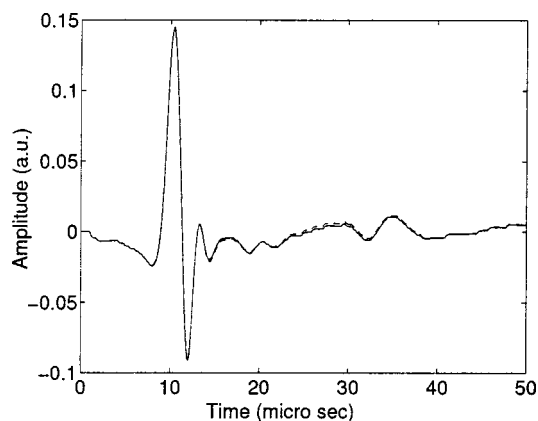


FIG. 3. Reflected wave at the first interface $x=0$ (solid line) and the total reflected wave (dashed line).

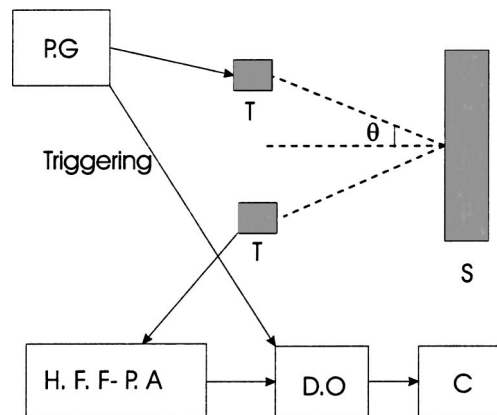


FIG. 4. Experimental set-up of the ultrasonic measurements in reflected mode P.G.: pulse generator, H. F. F. P. A.: high frequency filtering-pre-amplifier, D.O: digital oscilloscope, C: computer, T: transducer, S: sample.

different values of the incidence angle θ . The expression of the reflection coefficient at the first interface is given by

$$r(t, \theta) = \frac{\alpha_\infty \cos \theta - \phi \sqrt{\alpha_\infty - \sin^2 \theta}}{\alpha_\infty \cos \theta + \phi \sqrt{\alpha_\infty - \sin^2 \theta}} \delta(t). \quad (28)$$

For two values of the incidence angle θ_1 and θ_2 , it is easy to calculate the expression of the tortuosity function of the reflection coefficients $r_1 = r(t)|_{\theta_1}$ and $r_2 = r(t)|_{\theta_2}$ corresponding to the angles θ_1 and θ_2 , respectively,

$$\alpha_\infty = \frac{\left(\frac{(1-r_2)(1+r_1)\cos \theta_2}{(1+r_2)(1-r_1)\cos \theta_1} \right)^2 \sin^2 \theta_1 - \sin^2 \theta_2}{\left(\frac{(1-r_2)(1+r_1)\cos \theta_2}{(1+r_2)(1-r_1)\cos \theta_1} \right)^2 - 1}. \quad (29)$$

Knowing the value of the tortuosity, we deduce the expression of the porosity function of θ_i and r_i by the expression

$$\phi = \frac{\alpha_\infty (1-r_i) \cos \theta_i}{(1+r_i) \sqrt{\alpha_\infty - \sin^2 \theta_i}}, \quad i=1,2. \quad (30)$$

As an application of this model, some numerical simulations are compared to experimental results. Experiments are carried out in air with two broadband Ultrason NCT202

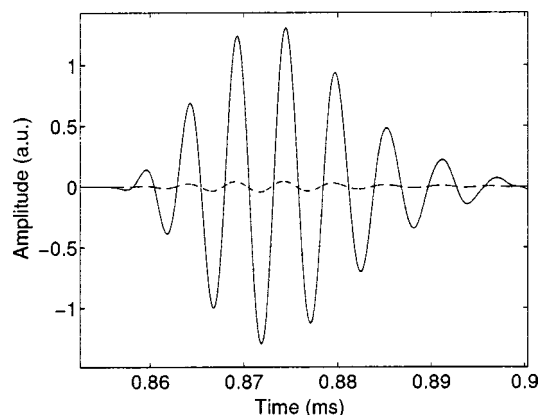


FIG. 5. Experimental incident signal (solid line) and experimental reflected signal (dashed line) by the material M2 ($\theta=0 \text{ deg}$).

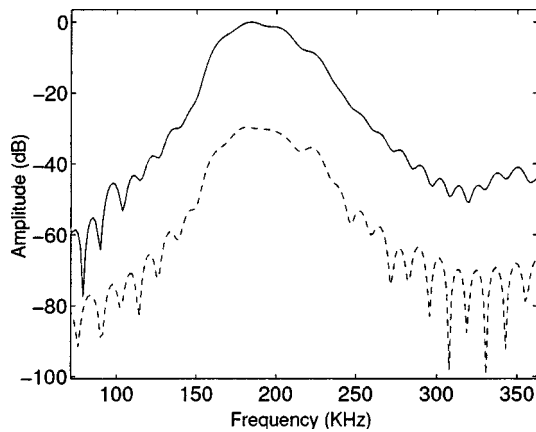


FIG. 6. Spectrum of experimental incident signal (solid line) and spectrum of experimental reflected signal (dashed line) for $\theta=0$ deg.

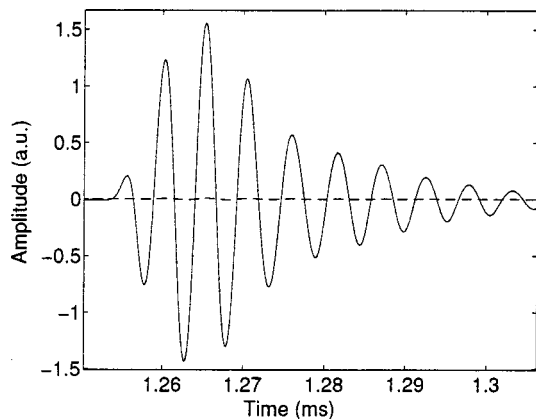


FIG. 7. Experimental incident signal (solid line) and experimental reflected signal (dashed line) by the material M2 ($\theta=53$ deg).

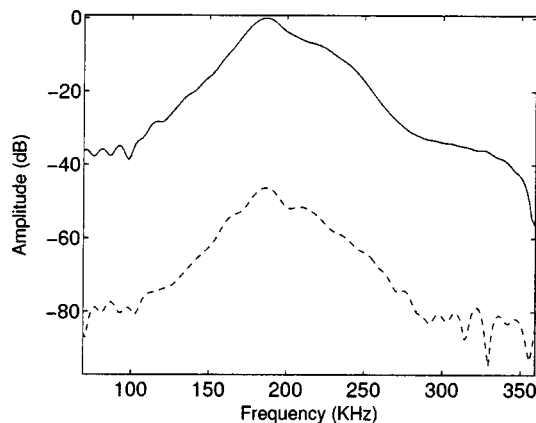


FIG. 8. Spectrum of experimental incident signal (solid line) and spectrum of experimental reflected signal (dashed line) for $\theta=53$ deg.

transducers having a 190 kHz central frequency in air and a bandwidth at 6 dB extending from 150 kHz to 230 kHz. A goniometer used in optic has been employed for the positioning of the transducers. Pulses of 400 V are provided by a 5052PR Panametrics pulser/receiver. The received signals are amplified up to 90 dB and filtered above 1 MHz to avoid high frequency noise. Electronic perturbations are removed by 1000 acquisition averages. The experimental setup is shown in Fig. 4. The distance between the transducers and the samples is 20 cm. The duration of the signal plays an important role, its spectrum must verify the condition of high frequency approximation referred to in the previous section.

The parameters of the first investigated plastic foam M2 are: resistivity $\sigma=2500 \text{ Nm}^{-4} \text{ s}$, thickness 4.1 cm, $\Lambda = 230 \mu\text{m}$, and $\Lambda' = 690 \mu\text{m}$. Figure 5 shows the incident signal generated by the transducer (solid line) and the reflected signal by the plastic foam M2 (dashed line) for normal incidence. Figure 6 shows their spectra. From the spectra of the two signals, the reader can see that they have practically the same bandwidth which means that there is no dispersion. The reflected signal from the foam M2 is very small compared with the incident signal because of the low value of its flow resistivity σ .

Figure 7 represents the incident signal generated by the transducer (solid line) and the reflected signal by the plastic foam M2 (dashed line) for an incidence angle $\theta=53$ deg. Figure 8 depicts their spectra, showing that there is also no dispersion in the diffusion process. This concurs with the theory below which predicts that the reflected wave from the first interface ($x=0$) is measured and simply attenuated by the factor $(\alpha_\infty \cos \theta - \phi \sqrt{\alpha_\infty - \sin^2 \theta}) / (\alpha_\infty \cos \theta + \phi \sqrt{\alpha_\infty - \sin^2 \theta})$. Table I gives the experimental data of the reflection coefficient for different values of the incidence angle θ and Table II give the values of the tortuosity and porosity calculated using of Eqs. (29) and (30) for each pair of incidence angles. The average value of the tortuosity obtained from these measurements is $\alpha_\infty = 1.07 \pm 0.09$ and the average value of the porosity is $\phi = 0.97 \pm 0.01$.

Figure 9 shows the experimental data of the reflection coefficient for different values of the incident angle θ , and the simulation of the variation of the reflection coefficient with the incident angle θ for the values of the tortuosity $\alpha_\infty = 1.07$ and porosity $\phi = 0.97$. The value of the porosity of the plastic foam M2 given by the porosimeter¹⁸ is $\phi = 0.98 \pm 0.02$, and the value of the tortuosity given by classical method^{1,3,4,19,21} is $\alpha_\infty = 1.06 \pm 0.08$. The reader can see the slight difference between the values of the porosity and tortuosity measured using this method and the other classical methods.^{1,3,4,18,19,21} Figure 10 shows the comparison between the simulated reflected signal at the first interface calculated for $\alpha_\infty = 1.07$ and $\phi = 0.97$, and the experimental reflected signal for $\theta=17$ deg. Figure 11 shows the same comparison for $\theta=53$ deg.

TABLE I. Experimental data of the reflection coefficient for different values of the incidence angle θ (foam M2).

Incidence angle θ (deg)	0	8	14	17	23	30	35	41	53.5
Reflection coefficient r	0.033	0.0326	0.0322	0.0315	0.0300	0.0265	0.025	0.0164	0.005

TABLE II. Values of the tortuosity and porosity calculated for each pair of incidence angles θ_1 and θ_2 (foam M2).

Incidence angle θ_1 / θ_2 (deg)	Tortuosity	Porosity
(a)		
0/8	1.080	0.976
0/14	1.054	0.961
0/17	1.068	0.967
0/23	1.07	0.969
0/30	1.086	0.975
0/35	1.071	0.968
0/41	1.100	0.981
0/53.3	1.039	0.954
8/14	1.039	0.954
8/17	1.063	0.965
8/23	1.069	0.968
8/30	1.085	0.975
8/35	1.070	0.968
8/41	1.100	0.981
8/53.5	1.069	0.968
14/17	1.099	0.980
14/23	1.081	0.972
14/30	1.081	0.972
14/35	1.073	0.969
14/41	1.104	0.982
14/53.5	1.070	0.977
(b)		
17/23	1.075	0.970
17/30	1.092	0.977
17/35	1.071	0.968
17/41	1.105	0.982
17/53.5	1.069	0.968
23/30	1.103	0.983
23/35	1.070	0.968
23/41	1.109	0.983
23/53.5	1.069	0.968
30/35	1.04	0.961
30/41	1.112	0.983
30/53.5	1.065	0.969
35/41	1.164	0.998
35/53.5	1.069	0.968
41/53.5	1.068	0.968

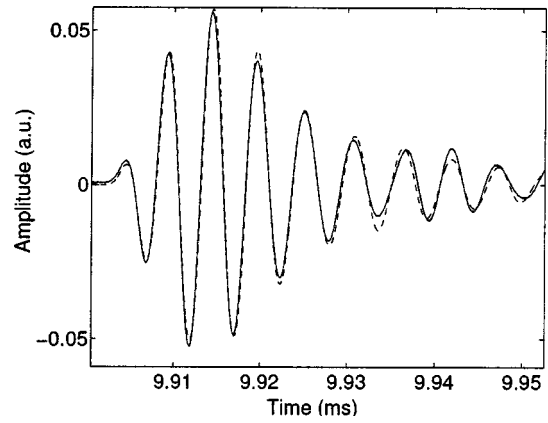


FIG. 10. Comparison between experimental reflected signal (solid line) and simulated reflected signal (dashed line) for M2 ($\theta=17$ deg).

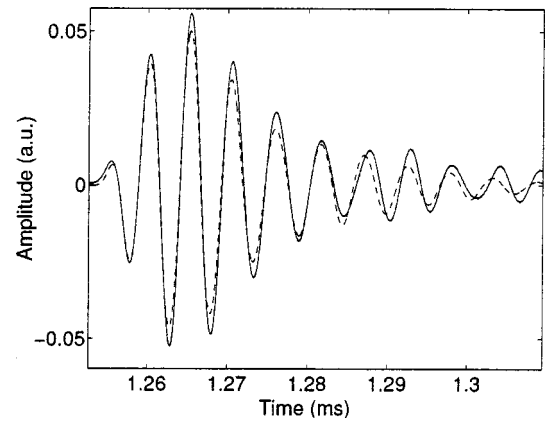


FIG. 11. Comparison between experimental reflected signal (solid line) and simulated reflected signal (dashed line) for M2 ($\theta=53$ deg).

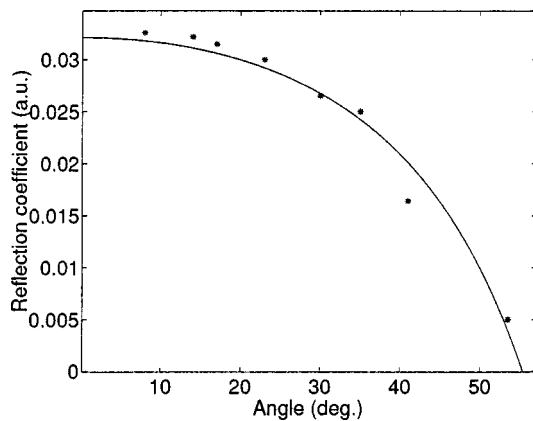


FIG. 9. Simulation of the variation of the reflection coefficient (solid line) with the incident angle θ and experimental data of the reflection coefficient (star) for the material M2.

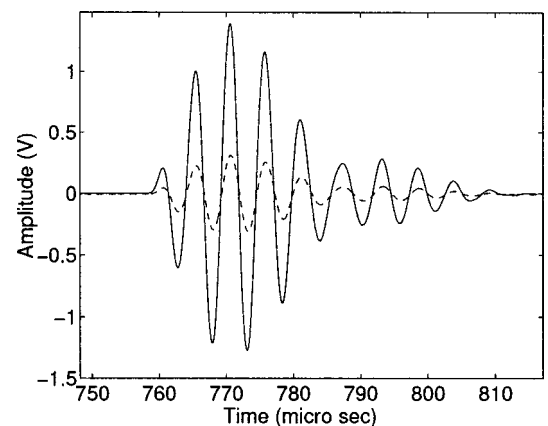


FIG. 12. Experimental incident signal (solid line) and experimental reflected signal (dashed line) by the material M3 for $\theta=13$ deg.

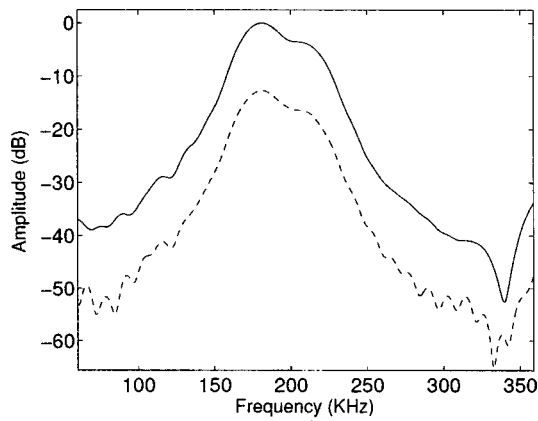


FIG. 13. Spectrum of experimental incident signal (solid line) and spectrum of experimental reflected signal (dashed line) for $\theta=13$ deg.

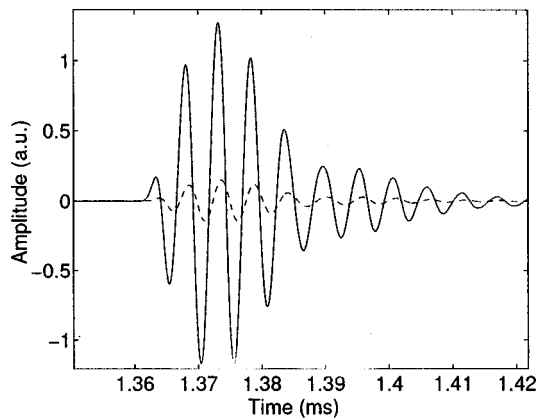


FIG. 14. Experimental incident signal (solid line) and experimental reflected signal (dashed line) by the material M3 for $\theta=49$ deg.

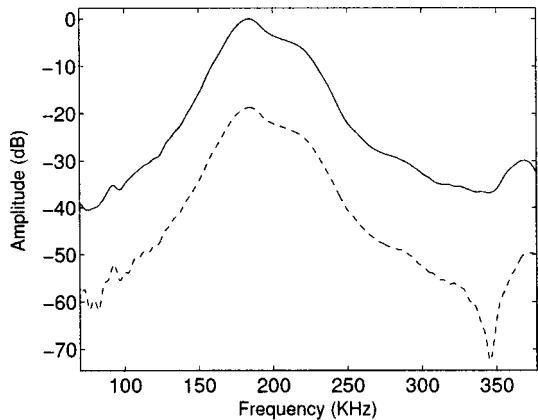


FIG. 15. Spectrum of experimental incident signal (solid line) and spectrum of experimental reflected signal (dashed line) for $\theta=49$ deg.

TABLE IV. Values of the tortuosity and porosity calculated for each pair of incidence angles θ_1 and θ_2 (foam M3).

Incidence angle θ_1 / θ_2 (deg)	Tortuosity	Porosity
(a)		
0/13.5	1.9	0.86
0/23	1.680	0.816
0/32.5	1.700	0.820
0/39.7	1.715	0.824
0/49.8	1.712	0.823
0/54	1.709	0.822
0/60.6	1.729	0.827
13.5/23	1.592	0.796
13.5/32.5	1.665	0.814
13.5/39.7	1.695	0.821
13.5/49.8	1.701	0.822
13.5/54	1.704	0.823
13.5/60.3	1.722	0.827
23/32.5	1.714	0.823
(b)		
23/39.7	1.729	0.826
23/49.8	1.719	0.824
23/54	1.719	0.824
23/60.3	1.735	0.828
32.5/39.7	1.743	0.829
32.5/49.8	1.72	0.824
32.5/54	1.721	0.824
32.5/60	1.739	0.828
39.7/49.8	1.709	0.823
39.7/54	1.713	0.824
39.7/60.3	1.738	0.821
49.8/54	1.695	0.829
49.8/60.3	1.761	0.829
54/60.3	1.801	0.832

The difference between the simulated reflected signal and experimental reflected signal is relatively weak which leads to the conclusion that the values of the tortuosity and porosity obtained are satisfactory.

Another plastic foam M3 (thickness 2.1 cm, $\Lambda = 23 \mu\text{m}$, and $\Lambda' = 69 \mu\text{m}$) with a higher value of the flow resistivity $\sigma = 125\,000 \text{ Nm}^{-4} \text{ s}$ has been investigated. Figure 12 shows the incident and reflected signals for $\theta=13$ deg and Fig. 13 shows their spectra. Here also, we can conclude from the two spectra that there is no dispersion. Figure 14 shows the incident and reflected signals for $\theta=49$ deg. Figure 15 shows their spectra. For this plastic foam M3, the reflected signal is more important than the one of the foam M2 because of its high value of the flow resistivity. The approximation that the reflected signal is essentially due to the reflection at the first interface is well verified in this case.

Table III gives the experimental data of the reflection coefficient for different values of the incidence angle θ and Table IV gives the values of the tortuosity and porosity calculated with Eqs. (29) and (30) for each pair of the incidence angles. The average value of the tortuosity obtained is $\alpha_\infty = 1.72 \pm 0.02$ and the average value of the porosity obtained

TABLE III. Experimental data of the reflection coefficient for different values of the incidence angle θ (foam M3).

Incidence angle θ (deg)	0	13.5	23	32.5	39.7	49.8	54	60.3
Reflection coefficient r	0.2274	0.221	0.2106	0.1905	0.1668	0.1163	0.0864	0.024

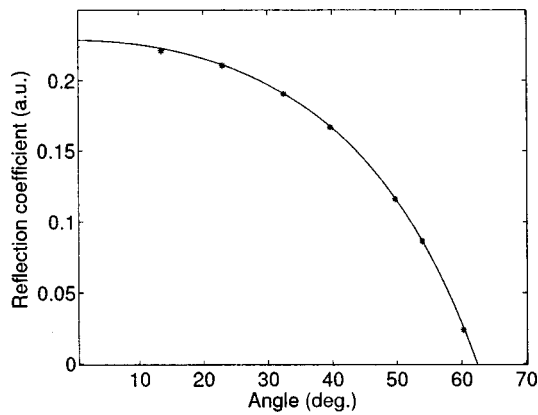


FIG. 16. Simulation of the variation of the reflection coefficient (solid line) with the incident angle θ and experimental data of the reflection coefficient (star) for the material M3.

is $\phi = 0.82 \pm 0.04$. Figure 16 shows the simulated variation of the reflection coefficient at the first interface for the value of the tortuosity $\alpha_\infty = 1.72$ and porosity $\phi = 0.82$ and experimental data of the reflection coefficient. The value of the porosity of the plastic foam M3 given by the porosimeter¹⁸ is $\phi = 0.8 \pm 0.1$, and the value of the tortuosity obtained by classical methods^{1,3,4,19,21} is $\alpha_\infty = 1.7 \pm 0.1$. Figure 17 shows the comparison between the simulated reflected signal at the first interface calculated for $\alpha_\infty = 1.72$ and $\phi = 0.8$, and the experimental reflected signal for $\theta = 13$ deg. The difference between the two results is small which leads to the conclusion that the values of the tortuosity and porosity obtained are satisfactory.

V. CONCLUSION

A method for the measurement of the porosity and the tortuosity simultaneously from the measurements of reflected waves at two oblique angles of incidence has been proposed. Generally, it is easy to evaluate the tortuosity from transmitted waves, this is not the case for porosity because of its weak sensitivity in transmitted mode. This method is an alternative to the usual method involving the use of a porosimeter

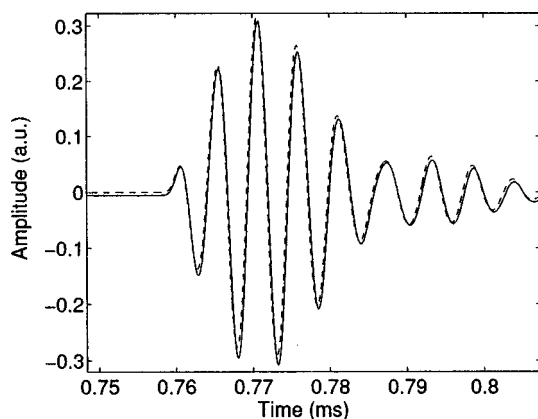


FIG. 17. Comparison between experimental reflected signal (solid line) and simulated reflected signal (dashed line) for M3 ($\theta = 13$ deg).

eter introduced by Beranek and improved by Champoux *et al.* or the other ultrasonic methods developed by Leclaire *et al.*

The method is based upon the propagation equation in time domain in a slab of porous material having a rigid frame at asymptotic domain (high frequency range). A time domain model of wave propagation in such material is worked out from the concept of fractional calculus. The kernels of the reflection and transmission scattering operators are derived giving simple relations between these operators and the parameters of the medium. Because of the high attenuation in such media, the reflected wave by the porous material can be approximated by the reflected wave at the first interface. As a consequence, it gives a simple relation between the porosity, tortuosity, incident angle and reflected wave, proving in such a way that all physical parameters of acoustic material can be evaluated from acoustic measurements.

An experimental validation of the theoretical expression of the reflection scattering operators illustrates the high level of correspondence between numerical and experimental results and show that this time domain model is well suited for the characterization of porous media via acoustic wave propagation.

ACKNOWLEDGMENT

The authors would like to express all thanks to the reviewers of the paper for their critical remarks.

- ¹Z. E. A. Fellah, M. Fellah, W. Lauriks, and C. Depollier, "Direct and inverse scattering of transient acoustic waves by a slab of rigid porous material," *J. Acoust. Soc. Am.* **113**, 61–73 (2003).
- ²Z. E. A. Fellah and C. Depollier, "Transient acoustic wave propagation in rigid porous media: A time-domain approach," *J. Acoust. Soc. Am.* **107**, 683–688 (2000).
- ³Z. E. A. Fellah, C. Depollier, and M. Fellah, "An approach to direct and inverse time-domain scattering of acoustic waves from rigid porous materials by a fractional calculus based method," *J. Sound Vib.* **244**, 359–366 (2001).
- ⁴Z. E. A. Fellah, C. Depollier, and M. Fellah, "Application of fractional calculus to the sound waves propagation in rigid porous materials: Validation via ultrasonic measurements," *Acust. Acta Acust.* **88**, 34–39 (2002).
- ⁵D. L. Johnson, J. Koplik, and R. Dashen, "Theory of dynamic permeability and tortuosity in fluid-saturated porous media," *J. Fluid Mech.* **176**, 379–402 (1987).
- ⁶J. F. Allard, *Propagation of Sound in Porous Media: Modeling Sound Absorbing Materials* (Chapman and Hall, London, 1993).
- ⁷M. A. Biot, "The theory of propagation of elastic waves in fluid-saturated porous solid. I. Low frequency range," *J. Acoust. Soc. Am.* **28**, 168–178 (1956).
- ⁸M. A. Biot, "The theory of propagation of elastic waves in fluid-saturated porous solid. II. Higher frequency range," *J. Acoust. Soc. Am.* **28**, 179–191 (1956).
- ⁹K. Attenborough, "Acoustical characteristics of porous materials," *Phys. Lett.* **82**, 179–227 (1982).
- ¹⁰L. L. Beranek, "Acoustic impedance of porous materials," *J. Acoust. Soc. Am.* **13**, 248–260 (1942).
- ¹¹C. Zwikker and C. W. Kosten, *Sound Absorbing Materials* (Elsevier, New York, 1949).
- ¹²Y. Champoux and J. F. Allard, "New empirical equations for sound propagation in rigid frame fibrous materials," *J. Acoust. Soc. Am.* **91**, 3346–3353 (1992).
- ¹³D. Lafarge, P. Lemarnier, J. F. Allard, and V. Tarnow, "Dynamic compressibility of air in porous structures at audible frequencies," *J. Acoust. Soc. Am.* **102**, 1995–2006 (1996).

- ¹⁴R. W. Leonard, "Simplified porosity measurements," *J. Acoust. Soc. Am.* **20**, 39–41 (1948).
- ¹⁵E. Guyon, L. Oger, and T. J. Plona, "Transport properties in sintered porous media composed of two particles sizes," *J. Phys. D* **20**, 1637–1644 (1987).
- ¹⁶D. L. Johnson, T. J. Plona, C. Scala, F. Psierb, and H. Kojima, "Tortuosity and acoustic slow waves," *Phys. Rev. Lett.* **49**, 1840–1844 (1982).
- ¹⁷J. Van Brakel, S. Modry, and M. Svata, "Mercury porosimetry: State of the art," *Powder Technol.* **29**, 1–12 (1981).
- ¹⁸Y. Champoux, M. R. Stinson, and G. A. Daigle, "Air-based system for the measurement of porosity," *J. Acoust. Soc. Am.* **89**, 910–916 (1991).
- ¹⁹P. Leclaire, L. Kelders, W. Lauriks, N. R. Brown, M. Melon, and B. Castagnède, "Determination of viscous and thermal characteristics lengths of plastic foams by ultrasonic measurements in helium and air," *J. Appl. Phys.* **80**, 2009–2012 (1996).
- ²⁰S. G. Samko, A. A. Kilbas, and O. I. Marichev, *Fractional Integrals and Derivatives: Theory and Applications* (Gordon and Breach Science, Amsterdam, 1993).
- ²¹N. Brown, M. Melon, V. Montembault, B. Castagnède, W. Lauriks, and P. Leclaire, "Evaluation of viscous characteristic length of air-saturated porous materials from the ultrasonic dispersion curve," *C. R. Acad. Sci. Paris*, **322**, 121–127 (1996).